

## PDF hosted at the Radboud Repository of the Radboud University Nijmegen

The following full text is a preprint version which may differ from the publisher's version.

For additional information about this publication click this link.

<http://hdl.handle.net/2066/124452>

Please be advised that this information was generated on 2018-07-07 and may be subject to change.

# Search for Free Gluons in Hadronic $Z^0$ Decays

The OPAL Collaboration

## Abstract

A search was performed for isolated, neutral, highly energetic particles which interact hadronically with matter. The data sample consists of 134 278 multihadronic events observed by the OPAL detector at LEP in  $e^+e^-$  collisions with centre-of-mass energies around the  $Z^0$  pole. Our study is sensitive to events predicted by a model in which gluons appear as free, stable, particles. We observed two events and derive a lower limit at 95% confidence level of 47 GeV on the barrier height  $V_m$  of a potential well introduced by this model. A Monte Carlo simulation of standard multihadronic  $Z^0$  decays predicts 3.3 events.

(Submitted to Physics Letters B)

# The OPAL Collaboration

P.D. Acton<sup>25</sup>, G. Alexander<sup>23</sup>, J. Allison<sup>16</sup>, P.P. Allport<sup>5</sup>, K.J. Anderson<sup>9</sup>, S. Arcelli<sup>2</sup>,  
P. Ashton<sup>16</sup>, A. Astbury<sup>a</sup>, D. Axen<sup>b</sup>, G. Azuelos<sup>18,c</sup>, G.A. Bahan<sup>16</sup>, J.T.M. Baines<sup>16</sup>,  
A.H. Ball<sup>17</sup>, J. Banks<sup>16</sup>, G.J. Barker<sup>13</sup>, R.J. Barlow<sup>16</sup>, J.R. Batley<sup>5</sup>, G. Beaudoin<sup>18</sup>,  
A. Beck<sup>23</sup>, J. Becker<sup>10</sup>, T. Behnke<sup>27</sup>, K.W. Bell<sup>20</sup>, G. Bella<sup>23</sup>, P. Berlich<sup>10</sup>, S. Bethke<sup>11</sup>,  
O. Biebel<sup>3</sup>, U. Binder<sup>10</sup>, I.J. Bloodworth<sup>1</sup>, P. Bock<sup>11</sup>, B. Boden<sup>3</sup>, H.M. Bosch<sup>11</sup>,  
S. Bougerolle<sup>b</sup>, B.B. Brabson<sup>12</sup>, H. Breuker<sup>8</sup>, R.M. Brown<sup>20</sup>, R. Brun<sup>8</sup>, A. Buijs<sup>8</sup>,  
H.J. Burckhart<sup>8</sup>, P. Capiluppi<sup>2</sup>, R.K. Carnegie<sup>6</sup>, A.A. Carter<sup>13</sup>, J.R. Carter<sup>5</sup>,  
C.Y. Chang<sup>17</sup>, D.G. Charlton<sup>8</sup>, P.E.L. Clarke<sup>25</sup>, I. Cohen<sup>23</sup>, W.J. Collins<sup>5</sup>, J.E. Conboy<sup>15</sup>,  
M. Cooper<sup>22</sup>, M. Couch<sup>1</sup>, M. Coupland<sup>14</sup>, M. Cuffiani<sup>2</sup>, S. Dado<sup>22</sup>, G.M. Dallavalle<sup>2</sup>,  
S. De Jong<sup>8</sup>, P. Debu<sup>21</sup>, L.A. del Pozo<sup>5</sup>, M.M. Deninno<sup>2</sup>, A. Dieckmann<sup>11</sup>, M. Dittmar<sup>4</sup>,  
M.S. Dixit<sup>7</sup>, E. Duchovni<sup>26</sup>, G. Duckeck<sup>11</sup>, I.P. Duerdoth<sup>16</sup>, D.J.P. Dumas<sup>6</sup>, G. Eckerlin<sup>11</sup>,  
P.A. Elcombe<sup>5</sup>, P.G. Estabrooks<sup>6</sup>, E. Etzion<sup>23</sup>, F. Fabbri<sup>2</sup>, M. Fincke-Keeler<sup>a</sup>,  
H.M. Fischer<sup>3</sup>, D.G. Fong<sup>17</sup>, C. Fukunaga<sup>24</sup>, A. Gaidot<sup>21</sup>, O. Ganel<sup>26</sup>, J.W. Gary<sup>4</sup>,  
J. Gascon<sup>18</sup>, R.F. McGowan<sup>16</sup>, N.I. Geddes<sup>20</sup>, C. Geich-Gimbel<sup>3</sup>, S.W. Gensler<sup>9</sup>,  
F.X. Gentit<sup>21</sup>, G. Giacomelli<sup>2</sup>, V. Gibson<sup>5</sup>, W.R. Gibson<sup>13</sup>, J.D. Gillies<sup>20</sup>, J. Goldberg<sup>22</sup>,  
M.J. Goodrick<sup>5</sup>, W. Gorn<sup>4</sup>, C. Grandi<sup>2</sup>, F.C. Grant<sup>5</sup>, J. Hagemann<sup>27</sup>, G.G. Hanson<sup>12</sup>,  
M. Hansroul<sup>8</sup>, C.K. Hargrove<sup>7</sup>, P.F. Harrison<sup>13</sup>, J. Hart<sup>5</sup>, P.M. Hattersley<sup>1</sup>,  
M. Hauschild<sup>8</sup>, C.M. Hawkes<sup>8</sup>, E. Heflin<sup>4</sup>, R.J. Hemingway<sup>6</sup>, R.D. Heuer<sup>8</sup>, J.C. Hill<sup>5</sup>,  
S.J. Hillier<sup>1</sup>, D.A. Hinshaw<sup>18</sup>, C. Ho<sup>4</sup>, J.D. Hobbs<sup>8</sup>, P.R. Hobson<sup>25</sup>, D. Hochman<sup>26</sup>,  
B. Holl<sup>8</sup>, R.J. Homer<sup>1</sup>, A.K. Honma<sup>e</sup>, S.R. Hou<sup>17</sup>, C.P. Howarth<sup>15</sup>, R.E. Hughes-Jones<sup>16</sup>,  
R. Humbert<sup>10</sup>, P. Igo-Kemenes<sup>11</sup>, H. Ihssen<sup>11</sup>, D.C. Imrie<sup>25</sup>, A.C. Janissen<sup>6</sup>,  
A. Jawahery<sup>17</sup>, P.W. Jeffreys<sup>20</sup>, H. Jeremie<sup>18</sup>, M. Jimack<sup>2</sup>, M. Jobes<sup>1</sup>, R.W.L. Jones<sup>13</sup>,  
P. Jovanovic<sup>1</sup>, D. Karlen<sup>6</sup>, K. Kawagoe<sup>24</sup>, T. Kawamoto<sup>24</sup>, R.K. Keeler<sup>a</sup>, R.G. Kellogg<sup>17</sup>,  
B.W. Kennedy<sup>15</sup>, C. Kleinwort<sup>8</sup>, D.E. Klem<sup>19</sup>, T. Kobayashi<sup>24</sup>, T.P. Kokott<sup>3</sup>,  
S. Komamiya<sup>24</sup>, L. Köpke<sup>8</sup>, J.F. Kral<sup>8</sup>, R. Kowalewski<sup>6</sup>, H. Kreutzmann<sup>3</sup>, J. von Krogh<sup>11</sup>,  
J. Kroll<sup>9</sup>, M. Kuwano<sup>24</sup>, P. Kyberd<sup>13</sup>, G.D. Lafferty<sup>16</sup>, F. Lamarche<sup>18</sup>, W.J. Larson<sup>4</sup>,  
J.G. Layter<sup>4</sup>, P. Le Du<sup>21</sup>, P. Leblanc<sup>18</sup>, A.M. Lee<sup>17</sup>, M.H. Lehto<sup>15</sup>, D. Lellouch<sup>26</sup>,  
P. Lennert<sup>11</sup>, C. Leroy<sup>18</sup>, J. Letts<sup>4</sup>, S. Levegrün<sup>3</sup>, L. Levinson<sup>26</sup>, S.L. Lloyd<sup>13</sup>,  
F.K. Loebinger<sup>16</sup>, J.M. Lorah<sup>17</sup>, B. Lorazo<sup>18</sup>, M.J. Losty<sup>7</sup>, X.C. Lou<sup>12</sup>, J. Ludwig<sup>10</sup>,  
M. Mannelli<sup>8</sup>, S. Marcellini<sup>2</sup>, G. Maringer<sup>3</sup>, A.J. Martin<sup>13</sup>, J.P. Martin<sup>18</sup>, T. Mashimo<sup>24</sup>,  
P. Mättig<sup>3</sup>, U. Maur<sup>3</sup>, J. McKenna<sup>a</sup>, T.J. McMahon<sup>1</sup>, J.R. McNutt<sup>25</sup>, F. Meijers<sup>8</sup>,  
D. Menszner<sup>11</sup>, F.S. Merritt<sup>9</sup>, H. Mes<sup>7</sup>, A. Michelini<sup>8</sup>, R.P. Middleton<sup>20</sup>, G. Mikenberg<sup>26</sup>,  
J. Mildenerberger<sup>6</sup>, D.J. Miller<sup>15</sup>, R. Mir<sup>12</sup>, W. Mohr<sup>10</sup>, C. Moisan<sup>18</sup>, A. Montanari<sup>2</sup>,  
T. Mori<sup>24</sup>, M.W. Moss<sup>16</sup>, T. Mouthuy<sup>12</sup>, B. Nellen<sup>3</sup>, H.H. Nguyen<sup>9</sup>, M. Nozaki<sup>24</sup>,  
S.W. O’Neale<sup>8,d</sup>, B.P. O’Neill<sup>4</sup>, F.G. Oakham<sup>7</sup>, F. Odorici<sup>2</sup>, M. Ogg<sup>6</sup>, H.O. Ogren<sup>12</sup>,  
H. Oh<sup>4</sup>, C.J. Oram<sup>e</sup>, M.J. Oreglia<sup>9</sup>, S. Orito<sup>24</sup>, J.P. Pansart<sup>21</sup>, B. Panzer-Steindl<sup>8</sup>,  
P. Paschievici<sup>26</sup>, G.N. Patrick<sup>20</sup>, S.J. Pawley<sup>16</sup>, P. Pfister<sup>10</sup>, J.E. Pilcher<sup>9</sup>, J.L. Pinfold<sup>26</sup>,  
D. Pitman<sup>a</sup>, D.E. Plane<sup>8</sup>, P. Poffenberger<sup>a</sup>, B. Poli<sup>2</sup>, A. Pouladdeh<sup>6</sup>, E. Prebys<sup>8</sup>,  
T.W. Pritchard<sup>13</sup>, H. Przysiezniak<sup>18</sup>, G. Quast<sup>27</sup>, M.W. Redmond<sup>9</sup>, D.L. Rees<sup>1</sup>, K. Riles<sup>4</sup>,  
S.A. Robins<sup>13</sup>, D. Robinson<sup>8</sup>, A. Rollnik<sup>3</sup>, J.M. Roney<sup>9</sup>, E. Ros<sup>8</sup>, S. Rossberg<sup>10</sup>,

A.M. Rossi<sup>2,f</sup>, M. Rosvick<sup>a</sup>, P. Routenburg<sup>6</sup>, K. Runge<sup>10</sup>, O. Runolfsson<sup>8</sup>, D.R. Rust<sup>12</sup>,  
S. Sanghera<sup>6</sup>, M. Sasaki<sup>24</sup>, C. Sbarra<sup>2</sup>, A.D. Schaile<sup>10</sup>, O. Schaile<sup>10</sup>, W. Schappert<sup>6</sup>,  
P. Scharff-Hansen<sup>8</sup>, P. Schenk<sup>a</sup>, H. von der Schmitt<sup>11</sup>, S. Schreiber<sup>3</sup>, J. Schwiening<sup>3</sup>,  
W.G. Scott<sup>20</sup>, M. Settles<sup>12</sup>, B.C. Shen<sup>4</sup>, P. Sherwood<sup>15</sup>, R. Shypit<sup>b</sup>, A. Simon<sup>3</sup>, P. Singh<sup>13</sup>,  
G.P. Siroli<sup>2</sup>, A. Skuja<sup>17</sup>, A.M. Smith<sup>8</sup>, T.J. Smith<sup>8</sup>, G.A. Snow<sup>17</sup>, R. Sobie<sup>g</sup>,  
R.W. Springer<sup>17</sup>, M. Sproston<sup>20</sup>, K. Stephens<sup>16</sup>, H.E. Stier<sup>10,†</sup>, R. Ströhmer<sup>11</sup>, D. Strom<sup>9</sup>,  
H. Takeda<sup>24</sup>, T. Takeshita<sup>24</sup>, P. Taras<sup>18</sup>, S. Tarem<sup>26</sup>, P. Teixeira-Dias<sup>11</sup>, N.J. Thackray<sup>1</sup>,  
G. Transtomer<sup>25</sup>, T. Tsukamoto<sup>24</sup>, M.F. Turner<sup>5</sup>, G. Tysarczyk-Niemeyer<sup>11</sup>, D. Van den  
plas<sup>18</sup>, R. Van Kooten<sup>8</sup>, G.J. VanDalen<sup>4</sup>, G. Vasseur<sup>21</sup>, C.J. Virtue<sup>19</sup>, A. Wagner<sup>27</sup>,  
C. Wahl<sup>10</sup>, J.P. Walker<sup>1</sup>, C.P. Ward<sup>5</sup>, D.R. Ward<sup>5</sup>, P.M. Watkins<sup>1</sup>, A.T. Watson<sup>1</sup>,  
N.K. Watson<sup>8</sup>, M. Weber<sup>11</sup>, P. Weber<sup>6</sup>, S. Weisz<sup>8</sup>, P.S. Wells<sup>8</sup>, N. Worms<sup>11</sup>,  
M. Weymann<sup>8</sup>, M.A. Whalley<sup>1</sup>, G.W. Wilson<sup>21</sup>, J.A. Wilson<sup>1</sup>, I. Wingerter<sup>8</sup>,  
V.-H. Winterer<sup>10</sup>, N.C. Wood<sup>16</sup>, S. Wotton<sup>8</sup>, T.R. Wyatt<sup>16</sup>, R. Yaari<sup>26</sup>, Y. Yang<sup>4,h</sup>,  
G. Yekutieli<sup>26</sup>, M. Yurko<sup>18</sup>, I. Zacharov<sup>8</sup>, W. Zeuner<sup>8</sup>, G.T. Zorn<sup>17</sup>.

<sup>1</sup>School of Physics and Space Research, University of Birmingham,  
Birmingham, B15 2TT, UK

<sup>2</sup>Dipartimento di Fisica dell' Università di Bologna and INFN, Bologna, 40126, Italy

<sup>3</sup>Physikalisches Institut, Universität Bonn, D-5300 Bonn 1, FRG

<sup>4</sup>Department of Physics, University of California, Riverside, CA 92521 USA

<sup>5</sup>Cavendish Laboratory, Cambridge, CB3 0HE, UK

<sup>6</sup>Carleton University, Dept of Physics, Colonel By Drive, Ottawa,  
Ontario K1S 5B6, Canada

<sup>7</sup>Centre for Research in Particle Physics, Carleton University, Ottawa,  
Ontario K1S 5B6, Canada

<sup>8</sup>CERN, European Organisation for Particle Physics, 1211 Geneva 23, Switzerland

<sup>9</sup>Enrico Fermi Institute and Department of Physics, University of Chicago,  
Chicago Illinois 60637, USA

<sup>10</sup>Fakultät für Physik, Albert Ludwigs Universität, D-7800 Freiburg, FRG

<sup>11</sup>Physikalisches Institut, Universität Heidelberg, Heidelberg, FRG

<sup>12</sup>Indiana University, Dept of Physics, Swain Hall West 117, Bloomington,  
Indiana 47405, USA

<sup>13</sup>Queen Mary and Westfield College, University of London, London, E1 4NS, UK

<sup>14</sup>Birkbeck College, London, WC1E 7HV, UK

<sup>15</sup>University College London, London, WC1E 6BT, UK

<sup>16</sup>Department of Physics, Schuster Laboratory, The University, Manchester, M13 9PL, UK

<sup>17</sup>Department of Physics and Astronomy, University of Maryland, College Park,  
Maryland 20742, USA

<sup>18</sup>Laboratoire de Physique Nucléaire, Université de Montréal, Montréal,  
Quebec, H3C 3J7, Canada

<sup>19</sup>National Research Council of Canada, Herzberg Institute of Astrophysics, Ottawa,

Ontario K1A 0R6, Canada

<sup>20</sup>Rutherford Appleton Laboratory, Chilton, Didcot, Oxfordshire, OX11 0QX, UK

<sup>21</sup>DPhPE, CEN Saclay, F-91191 Gif-sur-Yvette, France

<sup>22</sup>Department of Physics, Technion-Israel Institute of Technology, Haifa 32000, Israel

<sup>23</sup>Department of Physics and Astronomy, Tel Aviv University, Tel Aviv 69978, Israel

<sup>24</sup>International Centre for Elementary Particle Physics and Dept of Physics, University of Tokyo, Tokyo 113, and Kobe University, Kobe 657, Japan

<sup>25</sup>Brunel University, Uxbridge, Middlesex, UB8 3PH UK

<sup>26</sup>Nuclear Physics Department, Weizmann Institute of Science, Rehovot, 76100, Israel

<sup>27</sup>Universität Hamburg/DESY, II Inst. für Experimental Physik, 2000 Hamburg 52, FRG

<sup>a</sup>University of Victoria, Dept of Physics, P O Box 3055, Victoria BC V8W 3P6, Canada

<sup>b</sup>University of British Columbia, Dept of Physics, 6224 Agriculture Road,  
Vancouver BC V6T 1Z1, Canada

<sup>c</sup>Also at TRIUMF, Vancouver, Canada V6T 2A3

<sup>d</sup>On leave from Birmingham University, Birmingham B15 2TT, UK

<sup>e</sup>Univ of Victoria, Dept of Physics, P.O. Box 1700, Victoria BC V8W 2Y2, Canada and TRIUMF, Vancouver, Canada V6T 2A3

<sup>f</sup>Present address: Dipartimento di Fisica, Università della Calabria and INFN,  
87036 Rende, Italy

<sup>g</sup>University of British Columbia, Dept of Physics, 6224 Agriculture Road,  
Vancouver BC V6T 2A6, Canada and IPP, McGill University, High Energy Physics Department, 3600 University Str, Montreal, Quebec H3A 2T8, Canada

<sup>h</sup>On leave from Research Institute for Computer Peripherals, Hangzhou, China

<sup>†</sup>deceased 25th March 1991

Colour is generally assumed to be an unbroken symmetry in the Standard Model of the strong interaction. A number of searches for free quarks have been performed in order to test this assumption, and no free quark has been observed to date [1]. Like quarks, gluons are expected to appear only in colour singlet bound states. However, models exist in which colour is broken in such a way as to produce free gluons rather than free quarks [2, 3]. In one model  $SU(3)_C$  is spontaneously broken to  $SU(2) \times U(1)$  and contains one massless free gluon, which is a singlet of the new colour charge [2]. In this model the low-energy production of free gluons is suppressed by a short range confining potential of the form  $V(r) = 3sr e^{-\mu r}$ , where  $s$  is the string tension,  $r$  is the radial distance between the source and the gluon and  $\mu$  the typical range of the potential. The potential has a maximum  $V_m = 3s/e\mu$ .

The existence of high energy gluons was first established in  $e^+e^-$  annihilation events at centre-of-mass energies around 30 GeV [4]. The gluons in these events appeared as a third hadronic jet in addition to the two jets from the quark and antiquark. The multi-jet structure of hadronic events is even more apparent at the  $e^+e^-$  energies provided by LEP where the gluons radiated from the quarks are more energetic and more isolated. Together with the large production rate of multihadronic events at the  $Z^0$  peak, this makes LEP a good environment to study the properties of gluons and to search for free gluons.

In this paper we describe a search for free, stable, gluons as suggested in ref. [5] by selecting multihadronic events with isolated neutral particles which interact hadronically in the detector. The search is based on 134278 multihadronic events collected by OPAL at LEP during 1990 at centre-of-mass energies around the  $Z^0$  pole. We compare the results to predictions from the QCD plus hadronisation model JETSET[6], which is in excellent agreement with the properties and overall event shapes of our hadronic data sample [7].

As the OPAL detector has been described in detail in a recent publication [8], we restrict ourselves here to an overview of the main components. The coordinate system of the detector is defined with  $z$  along the beam direction,  $\theta$  and  $\phi$  being the polar and azimuthal angles. Tracking of charged particles is mainly performed by the jet chamber, a large volume drift chamber, 4 m long and 3.7 m in diameter, divided into 24 azimuthal sectors each containing a plane of 159 sense wires. The charge measured by the sense wires is used to obtain  $dE/dx$ , the energy loss of the particle in the detector gas. Together with the momentum, this gives a measurement of the particle's mass, leading to a  $\pi-K$  separating power of more than two standard deviations for momenta up to 20 GeV [9]. The jet chamber, a vertex detector, and chambers measuring the  $z$  coordinate of particles as they leave the jet chamber, are positioned inside a solenoidal coil which provides a uniform magnetic field of 0.435 T. It is surrounded by a time-of-flight counter array, a presampler and an electromagnetic calorimeter. The electromagnetic calorimeter consists of a barrel and two endcap arrays of lead glass blocks. Each block subtends a solid angle of approximately  $40 \times 40$  mrad<sup>2</sup>, with a thickness of over 24 radiation lengths in the barrel region and typically 22 radiation lengths in the endcaps. The energy resolution for

electrons of 45 GeV is typically  $\sigma_E/E \approx 3\%$ . The material in front of the presampler corresponds to  $\approx 2/\sin \theta$  radiation lengths. The presampler is designed to detect showers of particles originating in this material and consists of a cylinder of two layers of limited streamer mode chambers. Analogue readout of the wires and strips located on either side of the chambers yields a signal proportional to the number of traversing particles. The presampler multiplicity is defined as the ratio of this signal to the average signal from a non-showering particle. Outside the electromagnetic calorimeter is the instrumented return yoke of the magnet, forming the hadron calorimeter, and beyond this are the outer muon detectors. The hadron calorimeter, which consists of nine layers (eight layers in the endcap) of streamer tubes interleaved with the iron slabs of the magnet return yoke, is read out via 4 mm wide strips and projective towers formed from  $50 \times 50 \text{ cm}^2$  pads. These strips and pads provide measurements in the  $(r, \phi)$  plane and the  $z$  direction. The energy resolution of the bare hadron calorimeter was measured in test beams of 10 GeV pions to be  $\sigma_E/E \approx 120\%/\sqrt{E/\text{GeV}}$ . The material in front of the hadron calorimeter corresponds to about two hadronic interactions lengths.

The JETSET Monte Carlo (version 7.2 [6]) with parameters tuned to represent global event distributions at LEP energies [7] was used for the simulation of standard multihadronic  $Z^0$  decays. Events with free gluons were generated as follows: JETSET 7.2 Monte Carlo events were generated for the  $q\bar{q}g$  and  $q\bar{q}gg$  modes with a probability  $P$  for a gluon to escape the confining potential given by  $P = \Theta(E_t - V_m)\sqrt{1 - V_m/E_t}$  [5]. Here  $E_t$  is defined as the invariant mass of the free gluon and the quark which is nearest to it in momentum space, and  $\Theta$  is a step function. We assume that the gluon will have a pointlike interaction with matter [5]. This gives a geometrical cross section of  $\sigma \approx \sigma_0 A^{2/3}$  ( $A$  is the atomic number of the material), with  $\sigma_0 \approx 25 \text{ mb}$ . Since this is roughly comparable to the cross section for a  $K^0$ , we replaced the gluon in our Monte Carlo by a stable  $K_L^0$  for the simulation of the detector response. Since colour is still conserved in hadronic interactions, there will be a second coloured particle in one of the quark jets, which will be hard to detect due to the presence of the other charged and neutral hadrons in the jet. This second coloured particle was not simulated in the Monte Carlo. A sample of 163 189 standard JETSET events and samples of 500 events with free gluons, each at different values of  $V_m$ , were processed by code based on the GEANT package [10] in order to simulate the response of the OPAL detector. The events were subsequently processed by the standard event reconstruction programs. When compared to the data, the standard Monte Carlo event sample was always normalised to the 134 278 multihadronic events after an efficiency factor for the data of 0.98 was applied.

A characteristic signature for events with free, stable, gluons would be the presence of a highly energetic neutral particle, isolated from the two quark jets. We therefore searched for multihadronic  $Z^0$  decays with isolated hadronic clusters. Events with real  $K_L^0$ 's or neutrons are the background to this search, but they are expected to be produced rarely at large angles from the  $q\bar{q}$  system. Events were selected in three stages: *i*) the selection of multihadronic events, *ii*) the selection of events containing a low-multiplicity jet, and

iii) the selection of events with single isolated clusters of hadronic energy due to a neutral particle. A low-multiplicity jet is defined in this context as a jet in which the energy contributed by charged particles is small (less than 10% of the total jet energy). This intermediate selection was done in order to provide a sample of events with characteristics similar to the free gluon events, but with sufficient statistics to study systematic effects.

The first stage selection of multihadronic events was based on charged tracks. The pattern recognition program reconstructed charged tracks from strings of at least ten hits in the jet chamber. A good track was defined in this analysis as having: at least 30 hits registered in the jet chamber, the first one at a radius smaller than 75 cm; a distance of closest approach to the nominal beam axis of less than 1 cm, and  $|z| < 50$  cm at this point, and a momentum transverse to the beam axis of greater than 100 MeV. Multihadronic events were required to have more than four good tracks and a total scalar sum of the momenta of all good tracks greater than 15 GeV.

The second stage selection of the event sample was based on jets formed by clusters of electromagnetic and hadronic energy. An electromagnetic calorimeter (EC) cluster was defined as an energy deposition of more than 100 MeV in the barrel lead glass array, or more than 250 MeV in the endcap. In the endcap, which has a non-projecting geometry, a cluster was required to span at least two adjacent lead glass blocks. Hadron calorimeter (HC) clusters were energy depositions of more than 250 MeV recorded in the hadron calorimeter towers. In order to avoid noisy towers, an overlap was required with a strip signal of two or more hits. Furthermore, in order to reject spurious hits and electromagnetic showers which leak out of the back of the lead glass arrays, strip hits were required in at least two different layers of the calorimeter.

A jet finding algorithm [11] was applied to the electromagnetic and hadronic clusters separately. Charged tracks were not included. Clusters  $i$  and  $j$  were merged until  $y_{ij} = 2E_i E_j (1 - \cos \theta_{ij}) / (\sum_n E_n)$  exceeded  $y_{cut}$ . Here,  $E_i$  and  $E_j$  are the energies of the clusters  $i$  and  $j$ , respectively, and  $\theta_{ij}$  is the angle between them. The algorithm was applied to the electromagnetic calorimeter and the hadron calorimeter clusters separately, because the calorimeters have different spatial and energy resolutions.

The results of the jet finding algorithm are shown in figures 1a and b, where the jet rates are shown as a function of  $y_{cut}$  for EC and HC clusters. Only jets with  $|\cos \theta_{jet}| < 0.8$  were used in this analysis, where  $\theta_{jet}$  is the polar angle of the jet axis. The solid lines in figure 1 represent the results of the same jet finding algorithm applied to Monte Carlo simulations of standard multihadronic events. The jet rates observed in the hadron calorimeter alone are lower than the rate observed in the electromagnetic calorimeter, because low-energetic jets are fully absorbed in the lead glass and are not seen in the hadron calorimeter. Subsequently, HC jets were merged with EC jets if the angle between the EC and the HC jet axes was smaller than  $37^\circ$ . Figure 1c shows the relative rates of merged jets as a function of  $y_{cut}$ . Good agreement is observed between data and Monte



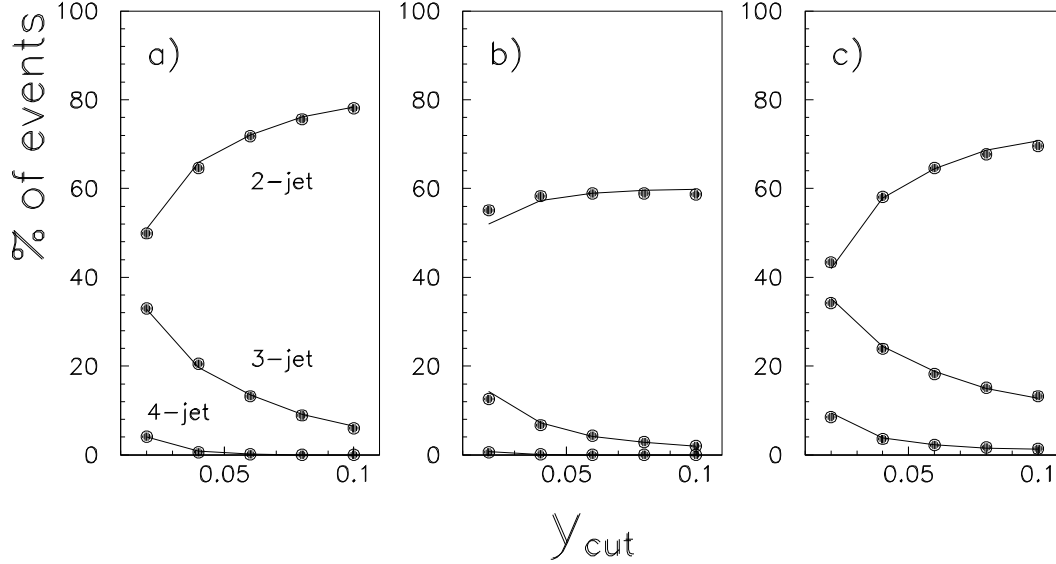


Figure 1: The rates of two-, three- and four-jet events as a function of  $y_{cut}$ , the cut-off parameter in the jet-finding algorithm, (a) using EC clusters only, (b) using HC clusters only, (c) after EC and HC jets were merged. The data are given as dots, the solid lines correspond to Monte Carlo simulations of standard multihadronic  $Z^0$  decays. Only jets with  $|\cos \theta_{jet}| < 0.8$  are counted in this figure.

Carlo events. For the following analysis we used  $y_{cut} = 0.06$ . A total energy  $E_{jet}$  was assigned to the merged jet, with  $E_{jet} = \alpha \times E_{ec} + E_{hc}$ . Here  $\alpha = 1.8$  is the measured  $e-\pi$  response ratio of the electromagnetic calorimeter, and  $E_{ec}$  and  $E_{hc}$  are the energies associated to the jets as observed in the EC and the HC, respectively. A jet cone with a half-opening angle of  $37^\circ$  was defined around the jet axis. This cone was used for the selection of low-multiplicity and neutral jets.

Events with low-multiplicity hadronic jets were selected with the following requirements. *i)* The polar angle of the jet had to satisfy  $|\cos \theta_{jet}| < 0.8$ . *ii)* The sum of the momenta of good charged tracks within the jet cone had to be less than 1 GeV. *iii)* The total jet energy  $E_{jet}$  had to be larger than 15 GeV. *iv)* At least 20% of the total jet energy had to be measured in the hadron calorimeter.

The distributions of low-multiplicity jets as functions of the total hadronic jet energy and of the ratio  $E_{hc}/E_{jet}$  are shown in figure 2. Only jets to which at least one HC cluster is associated enter in this plot. Figure 2a shows the event distributions as a function of  $E_{jet}$  for events with low-multiplicity jets passing all cuts except the cut  $E_{jet}$  for the data and for the standard Monte Carlo events. The histogram in figure 2b shows  $E_{jet}$  for

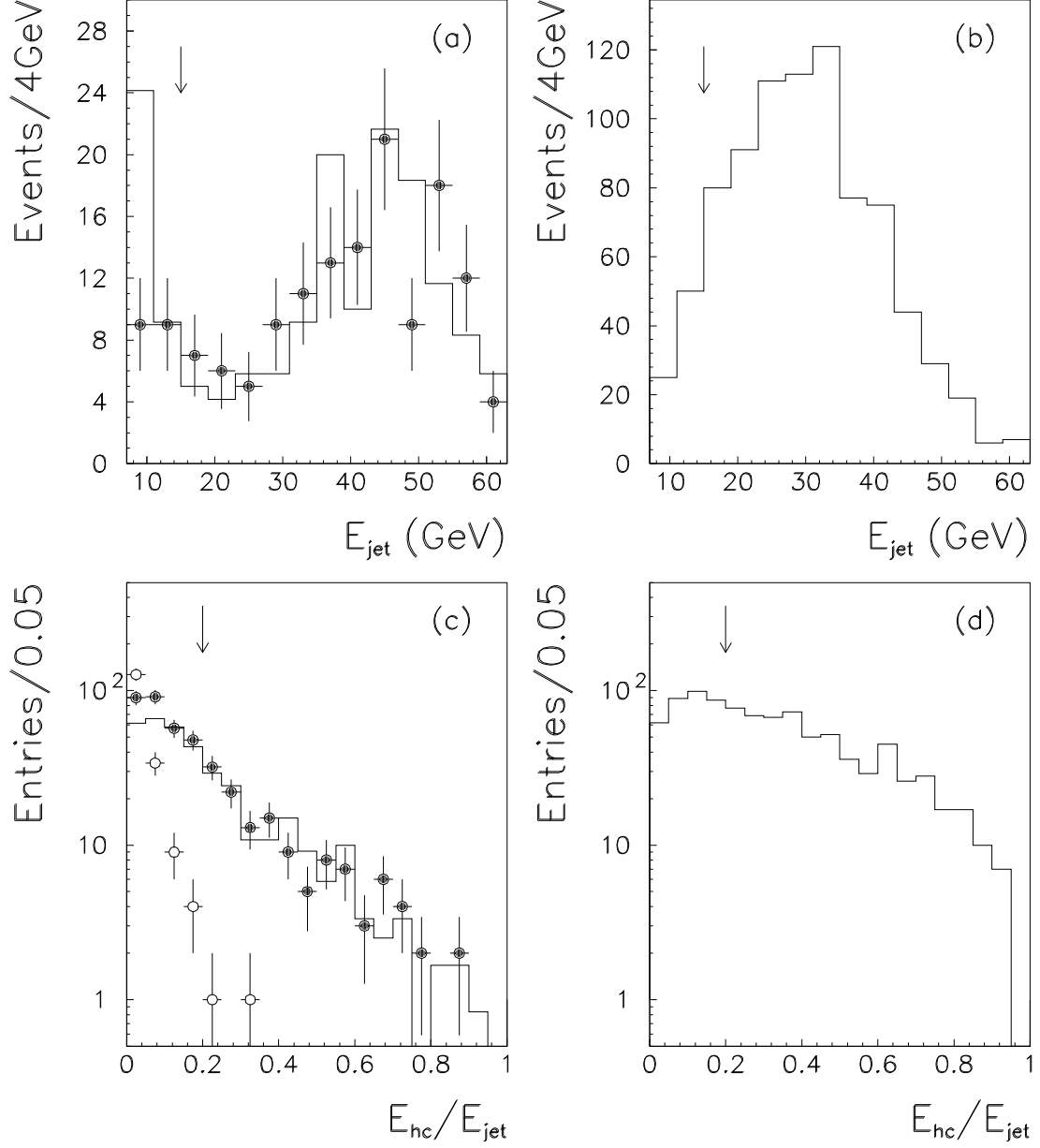


Figure 2: (a) The distribution of low-multiplicity jets as a function of the total hadronic jet energy  $E_{jet}$ . The points represent the data, the solid line represents the normalised standard multihadron Monte Carlo events. (b) The same distribution for events with free gluons generated at  $V_m = 30$  GeV. (c) The distribution of low-multiplicity jets as a function of  $E_{hc}/E_{jet}$ . The points and the solid line are defined as in (a). The open circles represent the distribution of 45 GeV electrons observed in the detector as a function of  $E_{hc}/E_{jet}$ . (d) The distribution for free gluon events generated at  $V_m = 30$  GeV. The arrows indicate where the cuts are applied for the following analysis.

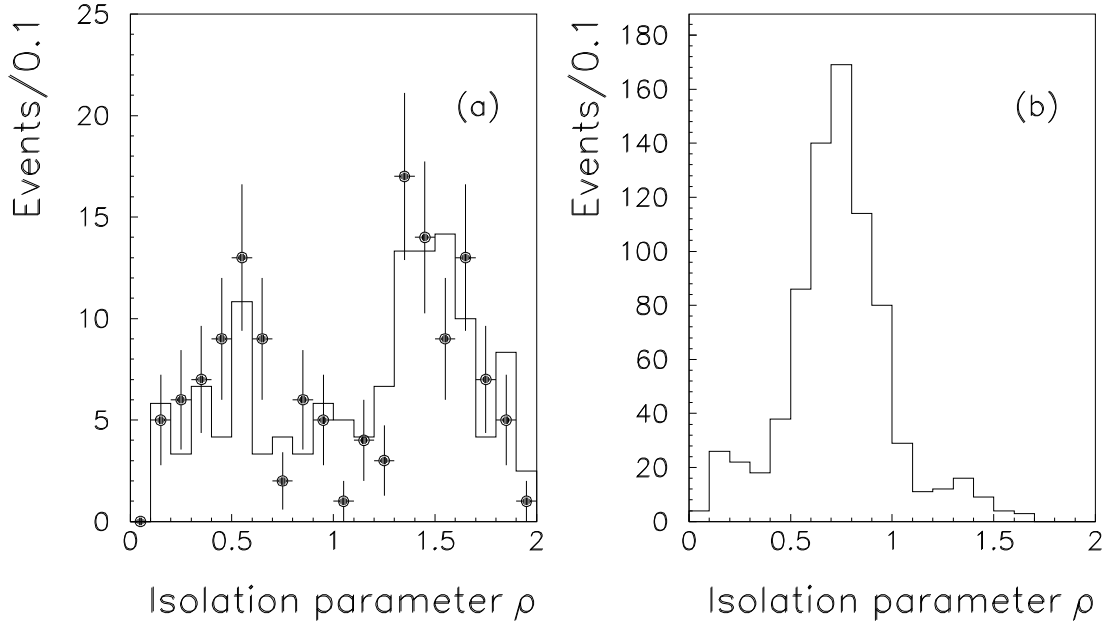


Figure 3: The distribution of events containing one low-multiplicity jet as a function of the isolation parameter  $\rho$ . The points in (a) represent the data, the solid line represents the normalised standard multihadron Monte Carlo events. (b) The same distribution for generated events with free gluons.

events generated with free gluons at  $V_m = 30$  GeV. Similarly, figures 2c and d show the distributions as a function of  $E_{hc}/E_{jet}$ . Above the cuts, the agreement between standard Monte Carlo events and data is reasonable.

In order to determine the effect of the cut on  $E_{hc}/E_{jet}$  on events with highly energetic isolated photons, the hadron calorimeter response to 45 GeV electrons from the reaction  $Z^0 \rightarrow e^+e^-$  observed in the detector was studied. For 176 out of 7730 electrons, an HC cluster as defined above was associated with the charged track. The open circles in figure 2c show the distribution of these electrons as a function of  $E_{hc}/E_{jet}$ . Only two electrons out of 7730 survived the cut  $E_{hc}/E_{jet} > 0.2$ . Since the showering properties of electrons and photons are very similar, we conclude that the background from photons in our final sample is negligible.

With these cuts 137 events were selected in the data and 131 events (after normalisation) in the standard multihadron Monte Carlo. In order to provide a reliability check on the global event shape of the events with low-multiplicity jets, we have defined an isolation parameter  $\rho$  as  $\rho = \min_{i \neq n} \sqrt{E_n E_i (1 - \cos \theta_{ni})} / E_{beam}$ . Here  $E_n$  and  $E_i$  are the energies of the low-multiplicity jet and every other jet  $i$  in the event, respectively, and  $\theta_{ni}$  is the angle between them. In figure 3a the distribution of the data events as a function of the isolation parameter is shown, together with the distribution of the standard Monte Carlo events. The structure between  $\rho = 1$  and  $\rho = 2$  is due to two-jet events, whereas the enhancement

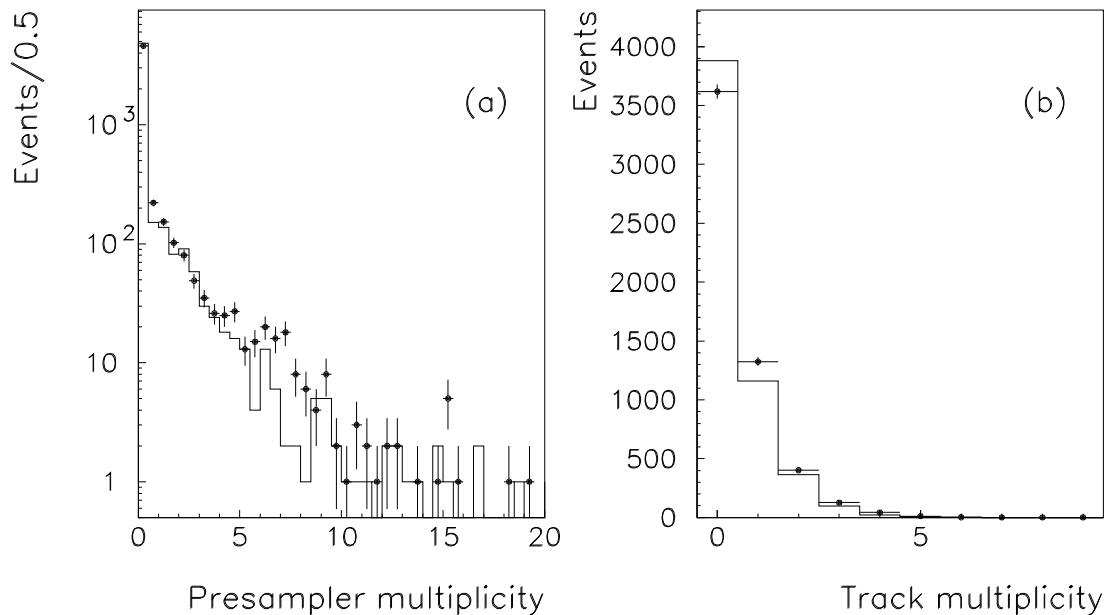


Figure 4: (a) The presampler and (b) the charged track multiplicities inside  $37^\circ$  cones containing no electromagnetic energy, randomly chosen in multihadron events. The points represent data, the solid lines represent the normalised standard multihadron Monte Carlo events.

below  $\rho = 1$  is due to three-jet events. Figure 3b shows the same distribution for the free gluon Monte Carlo events. The distribution peaks below  $\rho = 1$  as we expect from the three-jet nature of the free-gluon events.

We obtained the final event sample by applying the following additional cuts. *i)* There must not be any charged tracks within the jet cone in order to ensure that the hadronic energy cluster is solely due to neutral particles. *ii)* There must not be any signal observed in the presampler within the jet cone. Since the probability for a photon to initiate a shower in the magnet coil is approximately 80%, this cut suppresses cases in which the neutral non-showering particle is accompanied by one or more photons.

After the final cuts two events were observed in the data whereas four were found in the standard Monte Carlo sample, which after normalisation correspond to 3.3 events. The Monte Carlo events were due to a 43 GeV  $K_L^0$  in one event and isolated neutrons in the other three. In two of those the neutral cluster was caused by an isolated neutron-antineutron pair, in which the hadronic showers overlapped. The neutral hadrons in the data have values of  $\rho = 0.3$  and 1.3, the ones from the Monte Carlo have  $\rho = 0.5, 0.8, 0.8$  and 1.1.

We have estimated the systematic errors on the selection efficiency as a function of the barrier height  $V_m$  by varying the selection cuts. The dominant systematic errors arise from

| $V_m$<br>(GeV) | $\epsilon$<br>% | $(\Delta N_g/N_g)_\epsilon$<br>% | $(\Delta N_g/N_g)_{\Lambda_{\overline{MS}}}$<br>% | $(\Delta N_g/N_g)_{tot}$<br>% | $N_g^{exp}$ |
|----------------|-----------------|----------------------------------|---|-------------------------------|-------------|
| 30             | 17              | 26                               | 6.6   | 29                            | 102         |
| 40             | 17              | 22                               | 6.5   | 25                            | 27          |
| 45             | 20              | 22                               | 5.3   | 24                            | 13          |
| 50             | 18              | 23                               | 4.8   | 25                            | 4.6         |

Table 1: The reconstruction efficiencies  $\epsilon$ , the systematic errors on the selection efficiency  $(\Delta N_g/N_g)_\epsilon$ , the systematic errors due to the variation of  $\Lambda_{\overline{MS}}$ , the total errors on the numbers of expected events  $(\Delta N_g/N_g)_{tot}$ , and the numbers of expected events for different values of the barrier height  $V_m$ . The overall systematic errors also include the statistical errors of the generated event samples.

the cut on the energy fraction observed in the hadron calorimeter (15-18%) and the cut on the jet energy (8% at  $V_m = 45$  GeV). Systematic errors due to inadequate modelling of the detector response were estimated by comparing the effect of the cuts on the data with the effect of the cuts on the standard multihadron Monte Carlo events. The overall error in the simulation was estimated to be 12%.

In order to check the systematic effect of the two final cuts we selected in standard multihadron events 37° cones containing no electromagnetic energy. The presampler and track multiplicities inside these randomly chosen cones are shown in figures 4a and b. In the data we found 5% fewer cones with zero presampler multiplicity and 7% fewer cones with zero track multiplicity than in the Monte Carlo events, and we took these numbers as estimates of the systematic errors due to the cuts on these quantities. Together with the errors on the selection and the modelling of the data this gives a total systematic error of about 22%.

The systematic error for the production rate of free gluons was estimated by generating events for three values of  $\Lambda_{\overline{MS}}$ : 225, 345, and 140 MeV, which represent our measured value of  $\Lambda_{\overline{MS}}$  plus and minus one standard deviation, respectively [12]. The error obtained in this way is about 6%, depending on  $V_m$ . Table 1 summarises the selection efficiencies and systematic errors for different values of  $V_m$ . The last column shows the numbers of expected events with free gluons, for different values of the potential height  $V_m$ .

We have performed a cross check by selecting events in which we allowed one charged track of at least 15 GeV momentum and a presampler multiplicity compatible with a non-showering particle (multiplicity  $< 8$ ) in the jet cone. After rejecting obvious  $\tau^+\tau^-$  background we found seven such events. The standard Monte Carlo predicts nine events (7.4 after normalisation). Four of those are due to pions, four to protons and one to a kaon. Isospin symmetry predicts the number of (anti)protons to be equal to the number of (anti)neutrons and the number of charged kaons to be twice the number of  $K_L^0$ 's. Charged pions were not used in the comparison, since their isospin partners, the  $\pi^0$ 's, decay to

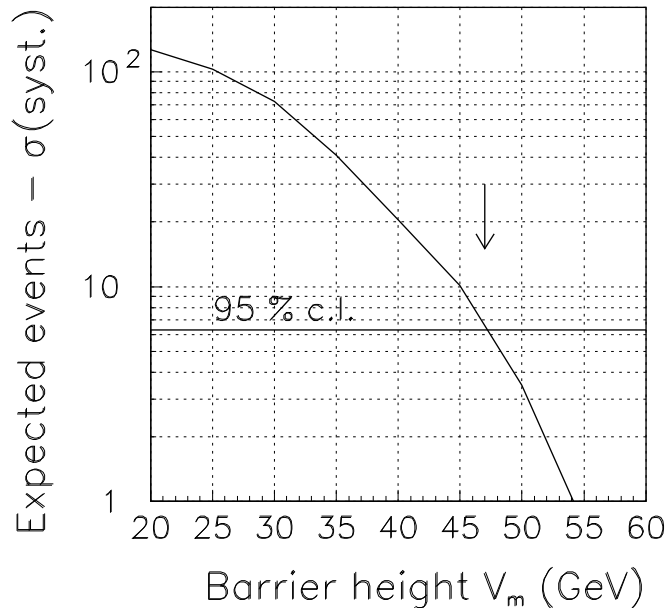


Figure 5: The number of expected events as a function of the barrier height  $V_m$  after subtraction of the systematic error in the selection efficiency. The horizontal line is the 95% confidence level limit on the maximum number of events observed.

photons which are rejected by the requirements on the hadron calorimeter. The  $dE/dx$  measurements in the jet chamber show that at least three of the highly energetic particles in the data events were compatible with being a kaon or a proton and incompatible with being pions. We conclude from this check that the Monte Carlo simulation is in good agreement with the data, and furthermore that the observed number of isolated neutral hadrons compares reasonably well with the corresponding number of charged hadrons.

As a further check, we have generated free gluon events at  $V_m = 45$  and  $50$  GeV in which the gluon was replaced by a neutron instead of by a kaon. The selection efficiency for these events was 18% in both cases. These efficiencies are slightly lower than those for events in which the gluon was replaced by a  $K_L^0$ , because the neutron has a higher probability of initiating a shower in the magnet coil and thus giving a signal in the presampler.

In order to set a conservative limit we have not made a background subtraction, but used the two data events to derive an upper limit at the 95% confidence level of 6.3 events for a possible signal. Subtracting one standard deviation in the total systematic error from the number of events expected after all cuts, we can exclude values of  $V_m$  lower than 47 GeV at the 95% confidence level, as shown in figure 5. The expected number of events continues to increase monotonically for lower values of  $V_m$  and hence all values of  $V_m$  lower than 47 GeV are excluded.

In conclusion, we have observed two events with an isolated highly energetic hadronic

cluster due to one or more neutral particles. From a Monte Carlo simulation using the Lund fragmentation scheme as implemented in JETSET 7.2 we expect 3.3 such events, demonstrating the validity of this model even for very rare event topologies. Comparing this result to a simple model in which the gluon radiated by one of the initial quarks materialises as a stable neutral particle with a hadronic interaction similar to a  $K_L^0$ , we find a lower limit of 47 GeV at 95% confidence level for  $V_m$ , a crucial parameter in this model.

## Acknowledgements

It is a pleasure to thank the SL Division for the efficient operation of the LEP accelerator, and its continuing close cooperation with our experimental group. In addition to the support staff at our own institutions we are pleased to acknowledge the Department of Energy, USA, the National Science Foundation, USA, the Science and Engineering Research Council, UK, the Natural Sciences and Engineering Research Council, Canada, the Israeli Ministry of Science, the Minerva Gesellschaft, the Japanese Ministry of Education, Science and Culture (the Monbusho) and a grant under the Monbusho International Science Research Program, the American Israeli Bi-national Science Foundation, the Direction des Sciences de la Matière du Commissariat à l'Energie Atomique, France, the Bundesministerium für Forschung und Technologie, FRG, the A.P. Sloan Foundation and the Junta Nacional de Investigação Científica e Tecnológica, Portugal.

## References

- [1] For a review of free quark searches, see:  
P. F. Smith, *Ann. Rev. Nucl. Part. Sci.* **39** (1989) 73;  
L. Lyons, *Phys. Rep.* **129** (1985) 225;  
M. Marinelli and G. Morpurgo, *Phys. Rep.* **85** (1982) 161.
- [2] R. Saly, M. K. Sundaresan and P. J. S. Watson, *Phys. Lett.* **115B** (1982) 239.
- [3] A. Shafer, B. Müller and W. Greiner, *Phys. Rev. Lett.* **50** (1983) 2047.
- [4] TASSO Collaboration, R. Brandelik et al., *Phys. Lett.* **86B** (1979) 243;  
PLUTO Collaboration, Ch. Berger et al., *Phys. Lett.* **86B** (1979) 418;  
MARK J Collaboration, D. P. Barber, *Phys. Rev. Lett.* **43** (1979) 830;  
JADE Collaboration, W. Bartel, *Phys. Lett.* **91B** (1980) 142.
- [5] R. L. Rinfret and P. J. S. Watson, *Phys. Lett.* **200B** (1988) 177.
- [6] T. Sjöstrand, *Comp. Phys. Comm.* **39** (1986) 347;  
M. Bengtsson and T. Sjöstrand, *Comp. Phys. Comm.* **43** (1987) 367;  
M. Bengtsson and T. Sjöstrand, *Nucl. Phys.* **B289** (1987) 810.
- [7] OPAL Collaboration, M. Z. Akrawy et al., *Z. Phys.* **C47** (1990) 505.
- [8] OPAL Collaboration, K. Ahmet et al., *Nucl. Instr. Meth.* **A305** (1991) 275.
- [9] M. Hauschild et al., CERN-PPE/91-130 (1991).
- [10] D. R. Ward, “The OPAL Monte Carlo Program – GOPAL”, presented at the MC91 Workshop, Amsterdam, The Netherlands, April 1991; to be published.
- [11] JADE Collaboration, W. Bartel et al., *Z. Phys.* **C33** (1986) 23;  
JADE Collaboration, S. Bethke et al., *Phys. Lett.* **213B** (1988) 235.
- [12] OPAL Collaboration, M. Z. Akrawy et al., *Z. Phys.* **C49** (1991) 375.